Al-Ni-NiO Pyrotechnic Time-Delays

Shasha Guo[a], Walter W. Focke*[a] and Shepherd M. Tichapondwa[a]

Abstract: The time delay elements in conventional mine detonators comprise pyrotechnic compositions pressed in aluminum tubes. Thermite and intermetallic reactions offer the possibility of greener alternatives for current heavy metal-based compositions. Unfortunately, the high reaction temperatures associated with conventional thermites cause operational failures due to the melting of the metal housings. Similarly, it is difficult to achieve sustained burning with intermetallic systems alone. Combination thermite-intermetallic systems may offer a solution to both problems. The concept is illustrated though ternary compositions based on powder mixtures of aluminum, nickel and nickel oxide. Progressive dilution of the primary thermite reaction, $5\ Al + 3\ NiO \rightarrow Al_2O_3 + 3\ AlNi$, with the intermetallic reaction, $Al + Ni \rightarrow AlNi$, smoothly reduced the adiabatic reaction temperature by as much as 800 K simultaneously maintaining consistent burn behavior inside both glass and lead tubes. However, in the process the burning rate gradually decreased from ca. 190 $mm \cdot s^{-1}$ to as low as 23 $mm \cdot s^{-1}$.

Keywords: Aluminum; nickel; nickel(II) oxide; thermite; intermetallic; time-delay

1 Introduction

Pyrotechnic compositions are energetic mixtures of oxidizers with reducing agents, optionally including binders and other functional components. Usually they burn relatively slowly to produce heat, color, light, smoke, gas, or sound [1]. They find application in numerous military and civilian devices [2]. The present interest is in environmentally friendly time delay compositions suitable for use as delay columns in mine detonators. This application requires both fast and slow burning systems to cover initiation delays ranging from milliseconds to several seconds. Some present delay compositions still rely on toxic heavy metal-based compounds. These need to be replaced with reliable, cost-effective and environmentally friendly alternatives.

A thermite is a pyrotechnic composition that produces high heat via a strongly exothermic reaction. The Al-Fe_2O_3 system is a classic example. On combustion, a metal oxide is reduced to its metal state by a less noble metallic fuel that, in turn, is converted into a more stable metal oxide [3]. Thermites employ fuel powders with high volumetric and gravimetric combustion enthalpies (e.g., Al, Mg, Mn, etc.) and metal-oxide powders such as Fe_2O_3, CuO, NiO, MoO_3, etc. Unfortunately, the high combustion temperatures of the classic thermites far exceed the melting points of the materials of construction used in detonator subassemblies. This precludes their direct use in conventional delay detonators. However, it should be possible to lower the reaction temperature to acceptable levels by including, either the product metal or the product metal oxide, in the thermite formulation. The present communication explores the effect of the former approach on the burning behavior of a ternary thermite mixture.

Aluminum is a particularly attractive metal fuel as it is safe and nontoxic, environmentally acceptable, inexpensive, and readily available in a variety of particle sizes and shapes. Unfortunately, it features a very high heat of combustion of $-31\ MJ \cdot kg^{-1}$ [4]. It also forms intermetallic compounds with other, nobler, metals, including nickel.

The characteristics of both micron- and nano-sized Al-NiO thermite systems, including the combustion mechanism, the effects of stoichiometry, particle sizes, compaction density, additives, etc., on the burning rate and product spectra are well-established [5]. In micron-scale thermites the ignition process is driven by a liquid-gas mechanism [6], the reaction is essentially gasless and the burning rate increases with compaction density [5b].

Similarly, the reactive intermetallic Ni-Al system has received considerable attention [7]. Diffusion plays a dominant role in this type of reactive system so that intimate phase contact is essential. Therefore, most studies considered Al-Ni laminates. However, stable burning was achieved employing composite particle laminates, e.g. micron-sized Al/Ni powder mixtures prepared by ball milling [8].

The Ni-Al binary phase diagram includes five intermetallic compounds, i.e. Al_3Ni, Al_3Ni_2, Al_3Ni_5, AlNi, and $AlNi_3$. The latter two are the most important and they are considered candidate materials for high temperature structural and coating applications [9]. Therefore, this study considered linear combinations of pure intermetallic and thermite reactions yielding either $AlNi_3$ or AlNi as intermetallic products. Figure 1, Scheme I and Scheme II show the details of the approach. Figure 1 shows the composition loci for the two linear blend systems defined by Schemes I and II. The thermochemistry of binary mixtures of Al+NiO, and compositions falling on these straight lines were explored. Sample mixtures were prepared and open-air burning and closed tube burning experiments were

[a] *S. Guo, W. W. Focke* and S. M. Tichapondwa*
IAM, Department of Chemical Engineering
University of Pretoria
Private Bag X20, Hatfield 0028, Pretoria, South Africa
E-mail: walter.focke@up.ac.za

conducted. The markers in **Figure 1** indicate successful ignition and burn experiments conducted inside filled glass tubes.

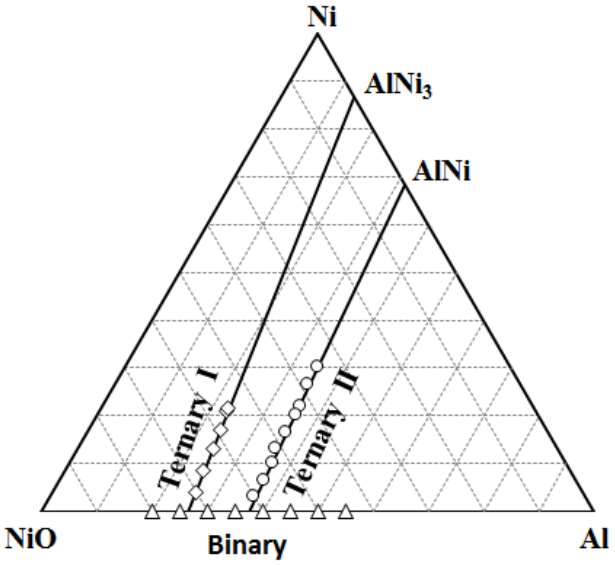

Figure 1. Experimental design showing the binary and ternary composition considered presently. The markers indicate compositions that ignited and burned sucessfully.

Table 1. Characteristics of the raw materials

Powder	Supplier	d_{50}[a] (µm)	BET[b] ($m^2 \cdot g^{-1}$)	Density ($g \cdot cm^{-3}$)
Al	Grinman	13.2 ± 0.03	0.34	2.70
Ni	SigmaAldrich	10.6 ± 0.03	0.24	8.91
NiO	SigmaAldrich	5.36 ± 0.05	0.76	6.67

[a]Volume-based mean particle size ± 1 SD. [b]BET surface area.

Ia: $3\ Al + 3\ NiO \rightarrow Al_2O_3 + AlNi_3$

Ib: $Al + 3\ Ni \rightarrow AlNi_3$

Netto: $(1+2x)Al + 3xNiO + 3(1-x)Ni \rightarrow xAl_2O_3 + AlNi_3$

Scheme I. Linear combination of thermite reaction Ia reaction with the $AlNi_3$ intermetalic reaction. The locus parameter x denotes the mass fraction of the reagents necessary for thermite reaction Ia. It is conveniently calculated from $x = 1/[1 + (M_{NiO}/M_{Ni})(w_{Ni}/w_{NiO})]$ where M_i and w_i are the molar mass and the mass fraction of component i in the initial mixture.

IIa: $5\ Al + 3\ NiO \rightarrow Al_2O_3 + 3\ AlNi$

IIb: $Al + Ni \rightarrow AlNi$

Netto: $(1+4y)Al + 3yNiO + (1-y)Ni \rightarrow yAl_2O_3 + (1+2y)AlNi$

Scheme II. Linear combination of the thermite reaction IIa with the AlNi intermetalic reaction. The locus parameter y is the mass fraction of the reagents required for the thermite reaction IIa. It is calculated from $y = 1/[1 + 3(M_{NiO}/M_{Ni})(w_{Ni}/w_{NiO})]$ where M_i and w_i are the molar mass and the mass fraction of component i in the composition.

2 Experimental Section

2.1 Materials

Table 1 lists the suppliers and the key characteristics of the raw powders used. All materials were used as received without further processing.

2.2 Preparation Methods

The compositions were prepared by a brush-mixing technique. Samples burned in 50 mm long borosilicate glass tubes were prepared as follows. Weighed-out reagent quantities were combined and repeatedly brushed through a 45-µm sieve. The resulting mixtures were loaded into the tubes and sealed at one end with a small piece of Prestik, a type of reusable putty. The inner/outer diameters of the two sets of tube were 4.0 mm/6.0 mm and 5.95 mm/8.0 mm respectively. Increments of the mixed powders (75±5 mg) were dispensed into the tubes. Repeated tapping consolidated the loaded powder to 40 ± 1% TMD before adding the next increment. The filling process was completed by topping the tube column off with a starter composition. This was a mixture of 10 wt-% Al, 20 wt-% Si, 20 wt-% Bi_2O_3 and 50 wt-% CuO. The starter quantities loaded were 25 mg and 70 mg for the 4.0 mm and 5.95 mm ID tubes respectively.

Samples burned in lead tubes were prepared in a similar fashion. Only two compositions were tested in this way. The starting tube lengths were 150 mm with OD = 11.5 mm and ID 7.0 mm. Composition amounts weighing 10.0 ± 0.3 g were tap-filled in the tube with the one end sealed. The composition in the tube was consolidated by a series of rolling operations on a proprietary tube-rolling machine. During each rolling operation, the sealed tube was passed through a hole with a smaller diameter. Compacted test samples with the inner tube diameters reduced to 5.5, 5.0 and 4.5 mm were obtained by applying four, five or six successive rolling steps respectively. The rolled lead tubes were then cut to a standard length of 40 ± 2 mm to form the delay elements. Then a portion of the composition was removed at one end to a depth of about 4 mm and replaced by the starter composition described above.

2.3 Characterization

The morphology of the powder particles was studied with a Zeiss Ultra Plus 55 scanning electron microscope (SEM) fitted with an In-Lens detector. The voltage setting was either 1 kV or 5 kV. The powders were carbon-coated with an Emitech K950X coater before scanning.

Particle size distributions and BET surface areas of the raw materials were determined with a Malvern Mastersizer 3000 and with a Micromeritics TriStar II 3020 respectively. X-ray diffraction (XRD) analyses were performed using a Bruker D8ADVANCE

instrument with 2.2 kW Cu long fine focus tube (Cu Kα, λ=1.54060). The system was equipped with a LynxEye detector with 3.7° active area. Samples were scanned from 2θ = 3° to 90° using a step size of 0.05° and with 5 s per step at generator settings of 40 kV and 40 mA. Data manipulation employed the Bruker DIFFRAC.EVA evaluation program. Before XRD analysis, the burn residue slags were milled into fine powders using a tungsten carbide mill.

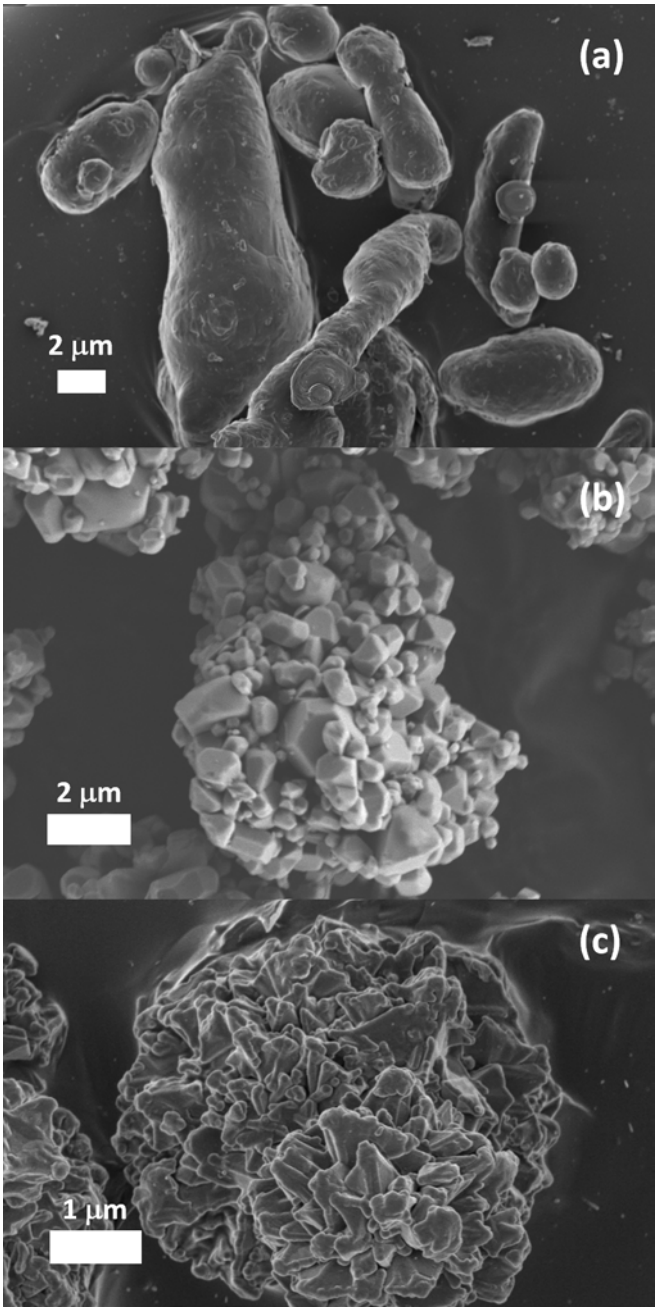

Figure 2. Scanning electron micrographs of the (a) aluminum, (b) nickel oxide, and (c) nickel particles.

2.4 Burning Rate Measurements

Open-air burns were conducted inside a fume hood. Grooves, 2 mm deep and 4 mm wide were machined into pyrophyllite blocks. The well-mixed powder was placed inside these slots and mildly compacted with the assistance of a small spatula. The sample burn length was set to about 40 mm. A small quantity of the starter composition was placed at one end and ignited with a butane torch.

The compacted lead tubes were suspended horizontally while the filled glass tubes were placed inside other, slightly larger, glass tubes serving as the horizontal holders. Ignition was triggered with an electrical fuse positioned in contact with the starter composition. The burning events were recorded with a digital camera at a frame rate of 240 Hz. The burning rate was estimated from the burn time, extracted from the video recording, and the effective burn length.

2.5 Modelling

Thermochemical simulations were carried out using the EKVI Release 4.30 thermodynamics software. The effect of mixture composition on the adiabatic reaction temperature, the product spectrum and the phase fractions, expected at this temperature, was analyzed.

3 Results and Discussion

3.1 Powder Characteristics

All the raw materials were found to be X-ray pure. The particle size and BET surface area results are listed in Table 1. SEM images and the XRD spectra of the Aluminum (Al), Nickel (Ni) and Nickel Oxide (NiO) powders are shown in Figure 2. The Ni and NiO powders actually consisted of agglomerates comprising much smaller primary crystalline particles. In case of the Al and Ni powders, approximately 12 vol.% of the particles were larger than 25 μm in size.

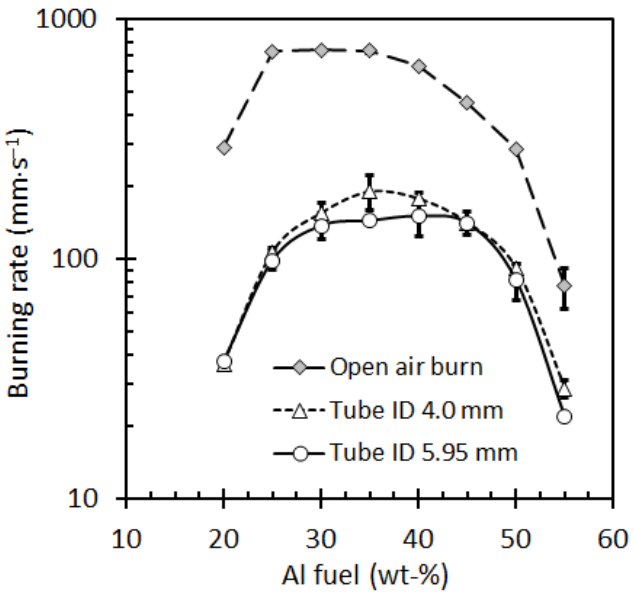

Figure 3. Open-air and glass tube linear burning rates for the Al-NiO binary system. The bulk density of the filled powder was ca. 40% TMD.

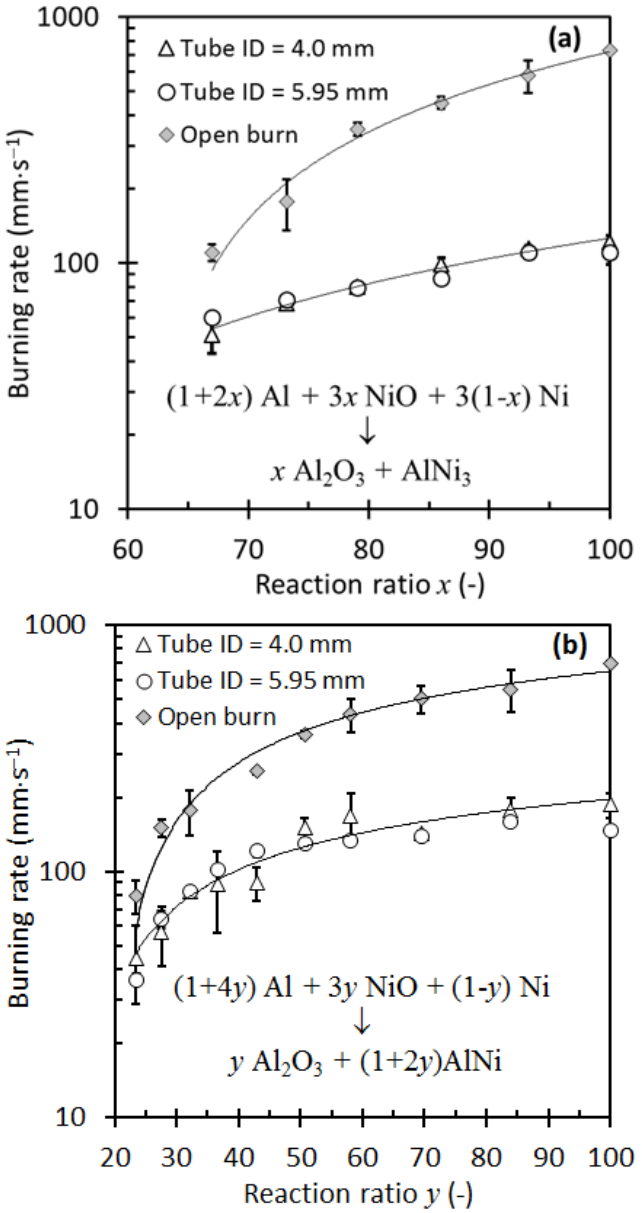

Figure 4. Linear burning rates measured in glass tubes for Al-NiO-Ni ternary systems generating (a) $AlNi_3$ and (b) AlNi as the target intermetallic products.

3.2 Burning Rates

Binary test compositions were prepared by varying the Al fuel content from 10 wt-% to 90 wt-%. Samples that ignited and burned successfully in glass tubes are shown plotted as discrete symbols in **Figure 1**. Of the binary thermite samples, only those containing 20 to 55 wt-% Al fuel burned as shown in **Figure 3.** The burning rates followed a near parabolic dependence on the Al fuel content and it was, within experimental error, independent of the tube diameter. The highest open-air burn rate was 740 ± 1 mm·s^{-1}. This was almost four times faster than the highest rate achieved in the 4.0 mm ID glass tube, i.e. 191 ± 31 mm·s^{-1}. The Al fuel content (ca. 37 wt-%) was consistent with the reaction $5Al + 3NiO \rightarrow Al_2O_3 + 3AlNi$.

Figure 4 presents the burning rates measured for the ternary mixtures. Again, the open burns proceeded much faster that those inside the packed glass tubes. The burning rates were also insensitive to the tube diameter. They decreased as the reagent compositions moved towards the neat intermetallic reaction, i.e. as the reactions ratios x and y decreased. Along the $AlNi_3$ locus, only samples containing at least two-thirds of the thermite reagents ignited and burned. However, for the AlNi intermetallic, sustained burning occurred over a wider composition range. The decrease in the burning rate with increasing contribution of the neat intermetallic was faster for the $AlNi_3$ system. The lowest sustainable burning rates were 45 ± 16 mm·s^{-1} and 36 ± 2 mm·s^{-1} for the $AlNi_3$ and AlNi ternary systems respectively.

Table 2 compares burning rates measured for samples filled into lead tubes to those recorded for open burns and samples filled into glass tubes. It reports data for both a binary and a ternary mixture. Compared to glass tubes, the burning rates measured in the lead tubes were somewhat slower. The unexpected result was the faster burning in the tubes with a smaller inner diameter. This was true for both the glass and the lead tubes. The reason for this are not currently understood.

The excessive heat generated by the binary mixture caused the lead to melt completely. This only happened after the very fast burning front had passed through. In contrast, the lead of the tubes containing the ternary mixture only partially melted. This was expected since this combination thermite-intermetallic system features a much lower adiabatic reaction temperature.

Table 2. The burning rates (mm·s^{-1}) of a binary and a ternary composition in the different types of delay elements

Type	ID × OD, mm	Binary[1]	Ternary[2]
Open[3]	4.0 × 2.0	734 ± 18	156 ± 6
Glass tubes	5.95 × 8.0	144 ± 5	65 ± 5
	4.0 × 6.0	191 ± 31	57 ± 16
Lead tubes	5.5 × 9.5	140 ± 7	46 ± 3
	5.0 × 9.0	172 ± 6	49 ± 2
	4.5 × 8.5	183 ± 20	48 ± 3

[1]Binary: 35 wt-%Al + 65 wt-% NiO; [2]Ternary: 60 wt-% (5Al+3NiO) + 40 wt-% (Al+Ni); [3]Width × depth; Compacted density in glass tubes and lead tubes were 40 ± 1% TMD and 54 ± 1% TMD respectively.

3.2 EKVI simulation and XRD results

Figure 5 shows the EKVI simulation results for binary mixtures of Al-NiO as a function of the Al fuel loading. Discussion of these results will focus on the Al composition range 20 wt-% to 55 wt-%. This corresponds to the sustainable combustion window determined experimentally. The adiabatic reaction temperature peaked at 3100 K for 19.8 wt-% Al as fuel consistent with the expected exothermic thermite reaction $2Al + 3NiO \rightarrow Al_2O_3 + 3Ni$. The temperature

plateau, at ca. 3090 K, between 20 wt-% and 38 wt-% Al is due to the progressive generation of the intermetallic AlNi (37.6 wt-% Al). Remarkably, the formation of $AlNi_3$ is not observed in the EKVI simulation. A possible reason is thermodynamic instability in the presence of the $NiAl_2O_4$ and Al_2O_3 phases. At even higher Al loadings, other intermetallic compounds formed. Beyond 40 wt-% Al in the feed, unreacted aluminum is present in the reaction mixture. Inside the sustainable combustion composition window, the reaction mixture is predominantly a liquid plus gas mixture (> 92 wt-% liquid) at the adiabatic reaction temperature. Predicted gas components included O_2, Ni, Al and Al_2O. However, negligible gas formation was observed in the actual burning experiments. The reaction temperatures likely never reached the theoretical adiabatic temperature extremes due to lateral heat losses.

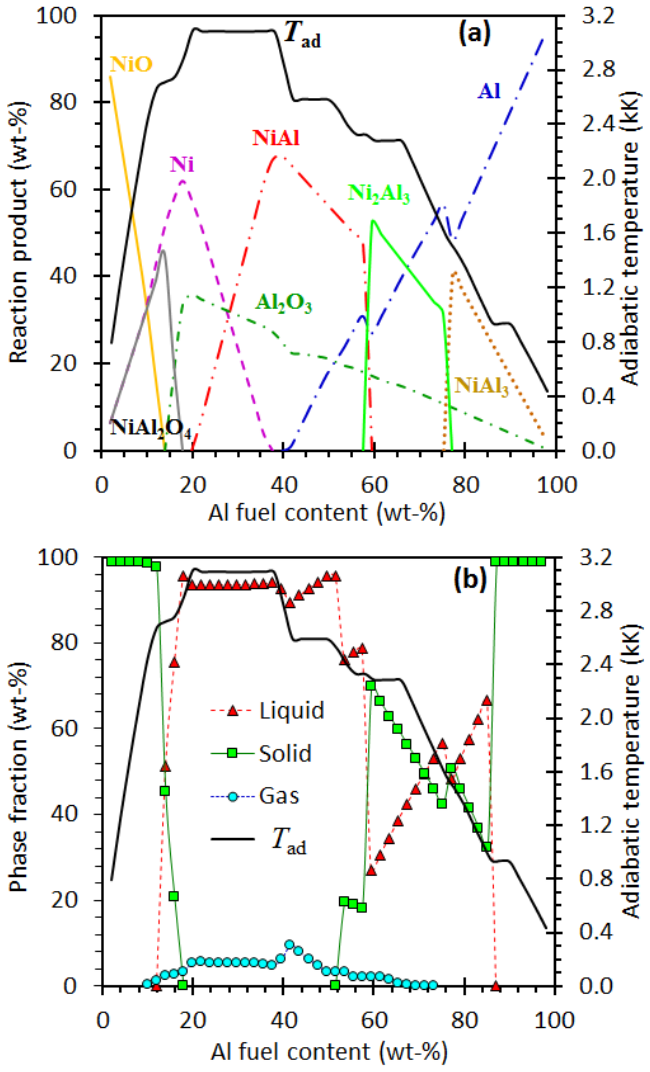

Figure 5. EKVI simulation results of the Al-NiO binary system: (a) adiabatic reaction temperature and condensed predicted products, (b) phase amount fraction.

Figure 6 reports XRD results for the burn residues recovered from glass tube after the combustion events. The tungsten carbide reflections are from contamination picked up during the slag milling process. Overall, the XRD results, for the Al-NiO binary system, are in qualitative agreement with the EKVI predictions. At 20 wt-% Al fuel the only products were Al_2O_3 (reflections at 2θ equal to 25.6°, 35.2° and 42.9°) and Ni metal (reflections at 2θ equal to 44.5° and 51.9°). The presence of the $AlNi_3$ phase (reflections at 2θ ≈ 44.1° and 51.1°) was evident in the residue obtained with 25 wt-% Al as fuel. This phase was replaced by AlNi (reflections at 2θ ≈ 31.4° and 44.5°) in the burn residue of the mixture made with 35 wt-% Al. At 50 wt-% Al as fuel, the presence of additional intermetallic phases, including Al_3Ni, AlNi and Al_3Ni_2, was observed.

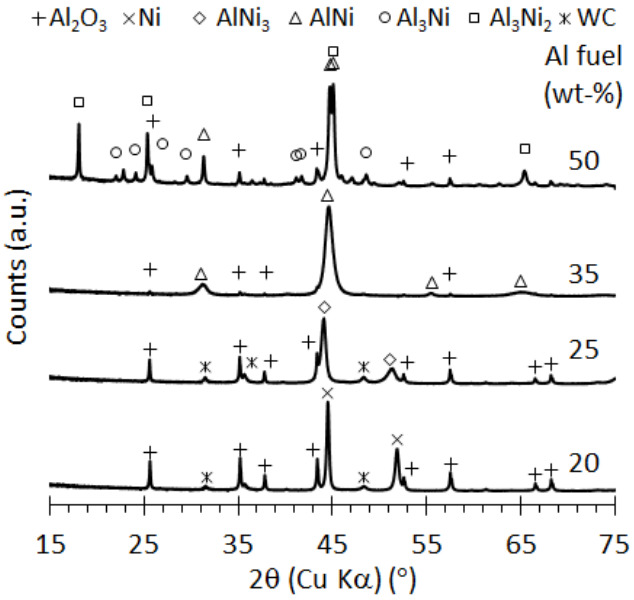

Figure 6. XRD reflections for the residues obtained after burning Al-NiO binary mixtures in glass tubes.

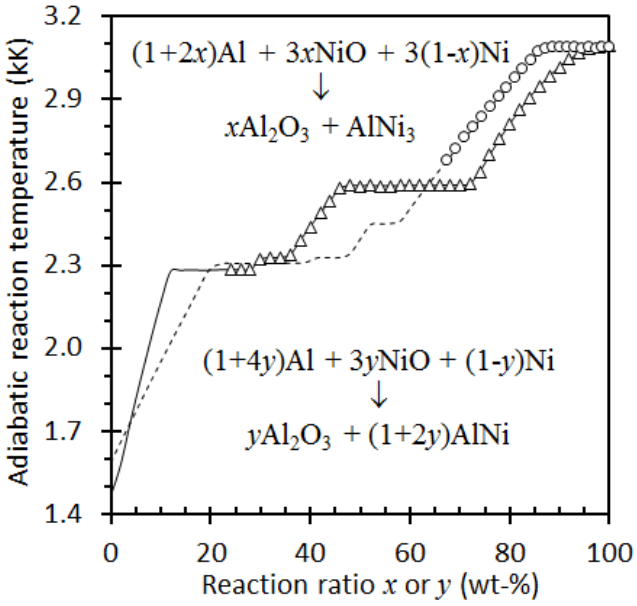

Figure 7. Effect of reaction blending on the EKVI-predicted adiabatic reaction temperature. The symbols

indicate the compositions capable of sustained burning in the $AlNi_3$ (-○-) and AlNi (–△–) ternary blend systems.

EKVI simulations for the Al-Ni binary system showed progressive formation of the expected intermetallic products $AlNi_3$, AlNi, Al_3Ni_2 and Al_3Ni as the Al fuel level was increased. Liquefaction of the reaction product commenced above 24 wt-% Al but no gas was evolved. The liquid fraction in the product reached a maximum of ca. 73 wt-% at 31.5 wt-% Al as fuel. This is consistent with the reaction $Al + Ni \rightarrow AlNi$. However, a higher adiabatic reaction temperature of 2200 K was attained at the 40.8 wt-% Al loading corresponding to Al_3Ni_2 as the main product.

Solid state combustion is self-sustaining only if the adiabatic reaction temperature exceeds a critical value estimated to be about 1800 K [10]. Figure 7 shows EKVI-predicted adiabatic reaction temperatures for the ternary mixtures along the composition loci shown in Figure 1. As expected, T_{ad} decreases with the parameters x and y. For the Ternary I blend, burning of the compositions failed once the predicted adiabatic reaction temperature decreased to below 2700 K. However, the Ternary II compositions only failed once T_{ad} dropped to below 2300 K.

XRD results were also obtained for the burn residues recovered from the combustion of the ternary compositions. They showed the presence of the expected combustion products. i.e. Al_2O_3 and either AlNi or $AlNi_3$. However, trace amounts of Al_3Ni_5 were detected in the residues for Ternary I.

4 Conclusion

The aluminum-nickel(II) oxide thermite system was adapted for potential use as a conventional pyrotechnic time delay system for mine detonators. EKVI thermodynamic simulations indicated a maximum adiabatic reaction temperature of 3100 K at an Al fuel content of 19.8wt-% consistent with the reaction

$$2\ Al + 3\ NiO \rightarrow Al_2O_3 + 3\ Ni$$

This temperature is too high for detonator time delay elements as lead or aluminum containments would melt.

It was possible to reduce the reaction temperature by up to 800 K by adding an additional amount of reagents that would react in an intermetallic fashion as for example $Al + Ni \rightarrow AlNi$. Burning rates were measured in borosilicate glass tubes with the compositions compacted to 40 ±1 % TMD and in lead tubes compacted to 54 ±1 % TMD. The highest burning rate (191 ± 31 $mm \cdot s^{-1}$) was measured in glass for a binary composition with 35 wt-% Al. XRD results confirmed that this composition conformed to the reaction $5\ Al + 3NiO \rightarrow Al_2O_3 + 3\ AlNi$. Adding $Al + Ni$ to this composition maintains the same reaction product, reduces the adiabatic reaction temperature and gently reduces the burning rate to much lower values. This composition successfully burned inside lead tubes at 46 – 48 $mm \cdot s^{-1}$. These results confirm that combination thermite-intermetallic reactions may have potential as time delay compositions in detonator trains.

Acknowledgements

This work is based on the research supported by the University of Pretoria through a bursary to S. Guo.

References

[1] G. Steinhauser, T. M. Klapötke. Using the chemistry of fireworks to engage students in learning basic chemical principles: a lesson in eco-friendly pyrotechnics. *Journal of Chemical Education* **2010,** *87* (2), 150-156.

[2] [a]B. Berger. Military pyrotechnics. *CHIMIA International Journal for Chemistry* **2004,** *58* (6), 363-368; [b]G. Steinhauser, T. M. Klapötke. "Green" pyrotechnics: a chemists' challenge. *Angewandte Chemie International Edition* **2008,** *47* (18), 3330-3347.

[3] [a]S. Knapp, N. Eisenreich, S. Kelzenberg, E. Roth, V. Weiser. Modelling of Al/MnO2 and Ti/MnO_2 Thermite Mixtures. *Propellants, Explosives, Pyrotechnics* **2019**; [b]E. L. Dreizin. Metal-based reactive nanomaterials. *Progress in energy and combustion science* **2009,** *35* (2), 141-167.

[4] J. Wang, A. M. Hu, J. Persic, J. Z. Wen, Y. N. Zhou. Thermal stability and reaction properties of passivated Al/CuO nano-thermite. *Journal of Physics and Chemistry of Solids* **2011,** *72* (6), 620-625.

[5] [a]G. Bohlouli-Zanjani, J. Z. Wen, A. Hu, J. Persic, S. Ringuette, Y. N. Zhou. Thermo-chemical characterization of a Al nanoparticle and NiO nanowire composite modified by Cu powder. *Thermochimica Acta* **2013,** *572*, 51-58; [b]S. W. Dean, M. L. Pantoya, A. E. Gash, S. C. Stacy, L. J. Hope-Weeks. Enhanced convective heat transfer in nongas generating nanoparticle thermites. *Journal of Heat Transfer* **2010,** *132* (11) Article 111201, pp 1-7.

[6] M. Fathollahi, H. Azizi-Toupkanloo. Thermal characterization and kinetic analysis of nano-and micro-Al/NiO thermites: Combined experimental and molecular dynamics simulation study. *Journal of the Chinese Chemical Society* **2019**, *66*, 909-918.

[7] [a]K. Morsi. Review: reaction synthesis processing of Ni–Al intermetallic materials. *Materials Science and Engineering: A* **2001,** *299* (1), 1-15; [b]C. Yeh, W. Sung. Combustion synthesis of Ni_3Al intermetallic compound in self-propagating mode. *Journal of Alloys and Compounds* **2004,** *384* (1-2), 181-191.

[8] C. E. Shuck, J. M. Pauls, A. S. Mukasyan. Ni/Al energetic nanocomposites and the solid flame phenomenon. *The Journal of Physical Chemistry C* **2016,** *120* (47), 27066-27078.

[9] K. Morsi. reaction synthesis processing of Ni–Al intermetallic materials. *Materials Science and Engineering: A* **2001,** *299* (1-2), 1-15.

[10] A. G. Merzhanov. Solid Flames: Discoveries, Concepts, and Horizons of Cognition. *Combustion Science and Technology* **1994,** *98* (4-6), 307-336.